IEEE Photonics Journal
An IEEE Photonics Society Publication

Open Access

A Frequency-Tunable Binary Phase-Coded Microwave Signal Generator With a Tunable Frequency Multiplication Factor

Volume 9, Number 6, December 2017

Yang Chen, *Member, IEEE*
Shilong Pan, *Senior Member, IEEE*

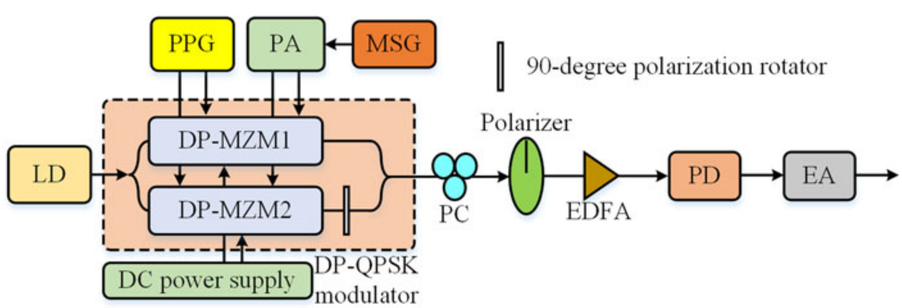

DOI: 10.1109/JPHOT.2017.2778419

A Frequency-Tunable Binary Phase-Coded Microwave Signal Generator With a Tunable Frequency Multiplication Factor

Yang Chen,[1] ***Member, IEEE***,
and Shilong Pan,[2] ***Senior Member, IEEE***

[1]School of Information Science and Technology, East China Normal University, Shanghai 200241, China
[2]Key Laboratory of Radar Imaging and Microwave Photonics, Ministry of Education, Nanjing University of Aeronautics and Astronautics, Nanjing 210016, China

DOI:10.1109/JPHOT.2017.2778419

Manuscript received October 19, 2017; revised November 20, 2017; accepted November 25, 2017. Date of publication November 29, 2017; date of current version December 14, 2017. This work was supported in part by the National Natural Science Foundation of China under Grant 61601297 and Grant 61422108, and in part by the Fundamental Research Funds for Central Universities. Corresponding author: Yang Chen (e-mail: ychen@ce.ecnu.edu.cn).

Abstract: A novel frequency-tunable binary phase-coded microwave signal generator with a tunable frequency multiplication factor is proposed. The key component of the proposed system is a dual-polarization quadrature phase-shift-keying (DP-QPSK) modulator, which is driven by the microwave reference signal and the coding signal. By properly controlling the bias points of the DP-QPSK modulator and the amplitudes of the microwave reference signal and the coding signal, a fundamental, frequency-doubled, frequency-tripled or frequency-quadrupled binary phase-coded microwave signal can be generated when two orthogonally polarized optical signals at the output of the DP-QPSK modulator are combined and then detected in a photodetector. The proposed system is experimentally evaluated. A binary phase-coded microwave signal is generated at the fundamental, doubled, tripled, or quadrupled frequency. The frequency tunability and the pulse compression performance of the generated phase-coded microwave signals are also experimentally studied.

Index Terms: Microwave photonics, phase coding, radar, DP-QPSK modulator, frequency multiplication.

1. Introduction

Pulse compression signals are widely used in modern radar system to achieve both large detection range and high range resolution [1], [2]. With the rapid development of radar systems, high-frequency or multifunction radars put forward new requirements for the generation of pulse compression signals, such as high frequency reachability, large frequency tunability, and large operating bandwidth. Conventionally, pulse compression signals are generated using electronic circuits, which leads to low operating frequency, small frequency-tunable range and limited operating bandwidth restricted mainly by the bandwidths of the electronic devices. As a result, pulse compression signals with high operating frequency, large frequency tunability and large operating bandwidth are very difficult or extremely expensive to be generated in the electrical domain.

Taking the advantage of large bandwidth offered by modern photonics, the generation of pulse compression signals using photonic technique has attracted great attentions in the past few years [3]–[5], which yields tremendous benefits, such as low loss, immunity to electromagnetic interference, large frequency tunability, large operating bandwidth and high operating frequency. Many optical systems have been proposed to generate pulse compression signals. A phase-coded or frequency-chirped microwave signal can be generated based on optical pulse shaping using a spatial light modulator (SLM) [6], which enables the generation of real-time updatable arbitrary microwave waveforms. However, the system is usually bulky due to the use of free-space optics. To reduce the volume and weight of the system, phase-coded or frequency-chirped microwave signals are generated using pure fiber optics, which avoids the transmission of optical signal in free space. In [7] and [8], pulse compression signals are generated based on optical spectral shaping and frequency-to-time mapping. The major disadvantage of this kind of technique is that the time duration of the generated pulse compression signal is usually limited to less than 1 μs, which limits its application in long-range measurement. External modulation is a promising technique to generate pulse compression signals with relatively long time duration. For instance, a binary phase-coded microwave signal has been generated using a Mach-Zehnder modulator (MZM) [9] or a dual parallel Mach-Zehnder modulator (DP-MZM) [10], by properly setting the amplitudes of the coding signal and the bias points of the modulator. To further increase the frequency of the generated phase-coded microwave signal, a frequency-doubled phase-coded microwave signal generator based on a polarization modulator (PolM) [11] and a frequency-quadrupled phase-coded microwave signal generator based on a dual-polarization quadrature phase shift-keying (DP-QPSK) modulator [12] are proposed. Another method to generate a pulse compression signal employing external modulation is realized by beating two phase-correlated optical wavelengths at a photodetector (PD) with the phase difference being controlled by the coding signal [13]–[17]. Using this method, we first need to generate two phase-correlated optical wavelengths, and then add the phase information onto the wavelengths. There are usually two ways to implement phase modulation on the two phase-correlated optical wavelengths: one is using an optical filter to filter out one optical wavelength and modulating the coding signal on it, which is then recombined with another optical wavelength [13], [14]; the other one is using a PolM to introduce complementary phase modulations to two orthogonally polarized optical wavelengths [15]–[17]. The approaches based on this principle are relatively complicated due to the use of an extra optical filter and a phase modulator (PM) or an extra PolM. Recently, we have proposed a phase-coded microwave signal generator with arbitrary phase modulation by using a single DP-QPSK modulator [18], which features very compact structure and great reconfigurability.

Most approaches mentioned above can only generate the phase-coded microwave signal at the fundamental frequency, which cannot meet the needs of high-frequency radar systems because the frequency range of the generated signal is limited. In [11], [12], and [17], frequency-multiplied phase-coded microwave signals can be generated, where high-frequency phase-coded microwave signals are generated using relatively low-frequency microwave reference signals. However, there are still some disadvantages associated with these approaches. In [11], the frequency multiplication factor is limited to two, though the structure of the system is very compact. In [12], the frequency multiplication factor reaches four, but the system is relatively complicated because the employment of a balanced detector besides the DP-QPSK modulator. In [17], high-frequency phase-coded microwave signals with a frequency multiplication factor of two, four or eight are generated, but the employment of an additional PolM besides the DP-QPSK modulator makes the system complicated. In addition, a fiber Bragg grating (FBG) is used to filter out the optical carrier when the frequency multiplication factor is eight, which influences the stability and the frequency tunability of the system. Furthermore, the approaches in [12] and [17] both employ electrical phase shifters, which are used to introduce phase differences between the microwave reference signals applied to the modulator. The limited bandwidth of the electrical phase shifter limits the operating frequency of the system. In addition, it is well known that phase-coded signal is a kind of vector signal. Recently, some approaches for frequency-multiplied vector signal generation in radio-over-fiber (ROF) system is proposed in [19] and [20]. The low-frequency vector signal is first generated in the electrical domain with an

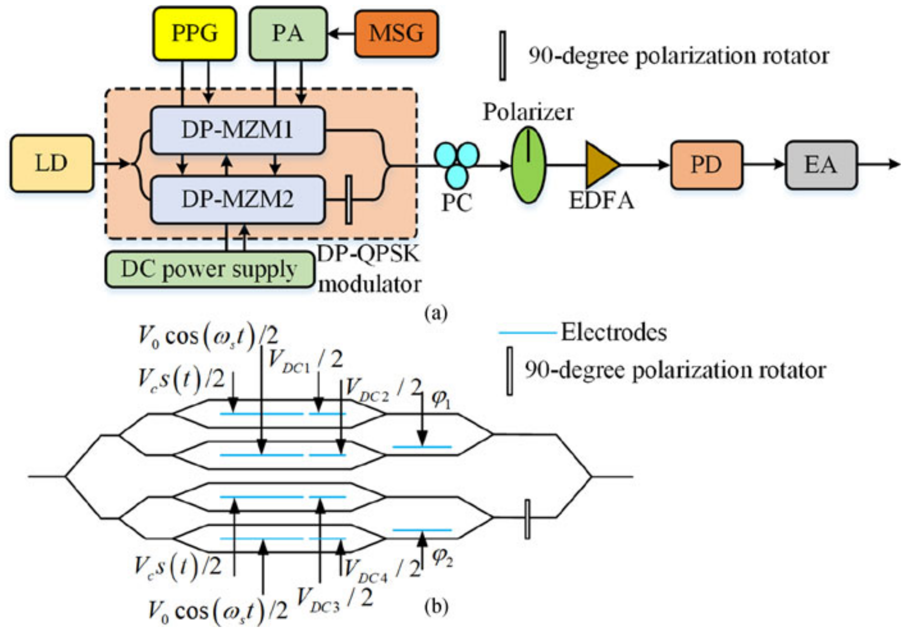

Fig. 1. (a) Schematic diagram of the proposed frequency-tunable phase-coded microwave signal generator. LD, laser diode; DP-MZM, dual-parallel Mach-Zehnder modulator; PC, polarization controller; EDFA, erbium-doped fiber amplifier; PD, photodetector; EA, electrical amplifier; PPG, pulse pattern generator; MSG, microwave signal generator; PA, power amplifier. (b) A diagram of how the electrical signals are applied to the DP-QPSK modulator.

additional pre-coding process, and then applied to optical modulators for frequency multiplication. However, these approaches are not optimal methods for the generation of phase-coded signals in radar system because the generation of the vector signal in the electrical domain limits the frequency-tunable range of the generated signal due to the limited bandwidth of the electronic circuits, and the pre-coding process makes the system relatively complicated.

In this paper, a phase-coded microwave signal generator with a tunable frequency multiplication factor from one to four is comprehensively studied in theory and verified by an experimental demonstration. The novel frequency-tunable binary phase-coded microwave signal generator mainly consists of a DP-QPSK modulator and a single-port PD with neither electrical phase shifters nor optical filters. The key contribution of the work is that the fundamental, frequency-doubled, frequency-tripled or frequency-quadrupled phase-coded microwave signal can be generated using the compact and reconfigurable structure. Due to insufficient power of the applied microwave reference signal in the experiment, an electrical band-pass filter is employed for frequency-quadrupled phase-coded microwave signal generation in this paper. However, this filter is not a necessary part of the system if enough microwave power can be achieved.

2. Principle of Operation

Fig. 1(a) shows the schematic diagram of the proposed frequency-tunable phase-coded microwave signal generator. A light wave generated from a laser diode (LD) with a fixed wavelength is injected into a DP-QPSK modulator. The DP-QPSK modulator consists of two DP-MZMs and a 90-degree polarization rotator. The coding signals generated from a pulse pattern generator (PPG) are applied to two RF ports of the DP-QPSK modulator. The microwave reference signal from a microwave signal generator (MSG) is amplified by a power amplifier (PA) and then applied to the other two RF ports of the DP-QPSK modulator. The six direct current (DC) bias ports of the DP-QPSK modulator are driven by DC power supplies. At the output of the DP-QPSK modulator, the two outputs from the two DP-MZMs are on the two orthogonal polarization states, respectively. The optical signals at the output of the DP-QPSK modulator is sent to a polarizer via a polarization controller (PC), and then amplified by an erbium-doped fiber amplifier (EDFA) before being detected in a single-port PD. The photocurrent from the PD is amplified by an electrical amplifier (EA). By properly adjusting the DC biases and the PC, a fundamental or frequency-multiplied binary phase-coded microwave signal is generated at the output of the PD.

Assuming the optical signal from the LD is $E_0 \exp(j\omega_c t)$, the microwave reference signal applied to the DP-QPSK modulator is $V_0 \cos(\omega_s t)/2$, and the coding signal applied to the DP-QPSK modulator is $V_c s(t)/2$, the optical signal at the output the DP-QPSK modulator can be expressed as

$$\begin{aligned}\begin{bmatrix} E_x(t) \\ E_y(t) \end{bmatrix} &= \frac{\sqrt{2}}{4}\alpha E_0 \begin{bmatrix} \cos\left(\frac{\pi V_c s(t) - \pi V_{DC1}}{2V_\pi}\right) + \cos\left(\frac{\pi V_0 \cos(\omega_s t) - \pi V_{DC2}}{2V_\pi}\right)\exp(j\varphi_1) \\ \cos\left(\frac{\pi V_c s(t) - \pi V_{DC3}}{2V_\pi}\right) + \cos\left(\frac{\pi V_0 \cos(\omega_s t) - \pi V_{DC4}}{2V_\pi}\right)\exp(j\varphi_2) \end{bmatrix} \exp(j\omega_c t) \\ &= \frac{\sqrt{2}}{4}\alpha E_0 \begin{bmatrix} \cos(\gamma s(t) - \theta_1) + \cos(\kappa\cos(\omega_s t) - \theta_2)\exp(j\varphi_1) \\ \cos(\gamma s(t) - \theta_3) + \cos(\kappa\cos(\omega_s t) - \theta_4)\exp(j\varphi_2) \end{bmatrix} \exp(j\omega_c t), \end{aligned} \tag{1}$$

where α represents the insertion loss the DP-QPSK modulator, E_0 and ω_c are the amplitude and the angular frequency of the optical signal, $V_0/2$ and ω_s are the amplitude and the angular frequency of the microwave reference signal, $s(t)$ is a bipolar coding signal $(+1, -1)$, $V_c/2$ is the amplitude of the coding signal, φ_1 and φ_2 are the phase shifts introduced in the two main-MZMs of the two DP-MZMs, V_π is the half-wave voltage of the DP-QPSK modulator, $\gamma = \pi V_c/2V_\pi$, $\kappa = \pi V_0/2V_\pi$, $\theta_i = \pi V_{DCi}/2V_\pi$, $V_{DCi}/2$ (i = 1, 2, 3, 4) is the DC bias voltage applied to the DP-QPSK modulator. Fig. 1(b) shows a diagram of how the electrical signals are applied to the DP-QPSK modulator.

Applying the optical signal at the output of the DP-QPSK modulator to a polarizer with its principal axis oriented at an angle of 45 degrees to one principal axis of the DP-QPSK modulator via tuning the PC, the optical signals on the two orthogonal polarization states are combined, which can be expressed as

$$\begin{aligned} E(t) &= \frac{\sqrt{2}}{2}E_x(t) + \frac{\sqrt{2}}{2}E_y(t) \\ &= \frac{1}{4}\alpha E_0 [2\cos A \cos(\gamma s(t) - B) + \cos(\kappa\cos(\omega_s t) - \theta_2)\exp(j\varphi_1) \\ &\quad + \cos(\kappa\cos(\omega_s t) - \theta_4)\exp(j\varphi_2)]\exp(j\omega_c t), \end{aligned} \tag{2}$$

where $A = (\theta_1 - \theta_3)/2$, $B = (\theta_1 + \theta_3)/2$.

Beating the optical signal from the polarizer at the PD, the photocurrent generated from the PD can be expressed as

$$\begin{aligned} i(t) = \frac{1}{16}R\alpha^2 E_0^2 \Big\{ & 1 + 4\cos^2 A \cos^2(\gamma s(t) - B) + \frac{1}{2}\cos(2\kappa\cos(\omega_s t) - 2\theta_2) \\ & + \frac{1}{2}\cos(2\kappa\cos(\omega_s t) - 2\theta_4) + 4\cos A \cos(\gamma s(t) - B) \\ & \times [\cos\varphi_1 \cos(\kappa\cos(\omega_s t) - \theta_2) + \cos\varphi_2 \cos(\kappa\cos(\omega_s t) - \theta_4)] \\ & + \cos(\varphi_1 - \varphi_2)[\cos(\theta_2 - \theta_4) + \cos(2\kappa\cos(\omega_s t) - \theta_2 - \theta_4)]\Big\}, \end{aligned} \tag{3}$$

where R is the responsivity of the PD. When $\theta_2 = \pi/2$ and $\theta_4 = 0$ establish, Eq. (3) can be simplified as

$$\begin{aligned} i(t) = \frac{1}{16}R\alpha^2 E_0^2 \Big\{ & \underbrace{1}_{1st} + \underbrace{4\cos^2 A \cos^2(\gamma s(t) - B)}_{2nd} + \underbrace{4\cos A \cos(\gamma s(t) - B)}_{3rd} \\ & \underbrace{\times [\cos\varphi_1 \sin(\kappa\cos(\omega_s t)) + \cos\varphi_2 \cos(\kappa\cos(\omega_s t))]}_{3rd} + \underbrace{\cos(\varphi_1 - \varphi_2)\sin(2\kappa\cos(\omega_s t))}_{4th} \Big\}. \end{aligned} \tag{4}$$

The first and second terms in Eq. (4) are a DC and a baseband modulation product, respectively, and the third term is a microwave signal modulated by the coding signal. The fourth term in Eq. (4) is a pure microwave signal. In order to generate a phase-coded microwave signal, the fourth term in Eq. (4) should be suppressed, and the third term is the phase-coded microwave signal we desire.

When $\varphi_1 = 0$ and $\varphi_2 = \pi/2$, Eq. (4) can be simplified as

$$i(t) = \frac{1}{16} R\alpha^2 E_0^2 \left\{1 + 4\cos^2 A \cos^2(\gamma s(t) - B) + 4\cos A \cos(\gamma s(t) - B) \sin(\kappa \cos(\omega_s t))\right\}. \quad (5)$$

As can be seen from Eq. (5), at the output of the PD, only a DC and a baseband modulation product besides the microwave modulation term are generated. Since the DC and the baseband component cannot be radiated to free space due to the band-pass characteristic of the radar transmit antenna, they can be ignored. Because $s(t)$ is a bipolar signal, we set $A = 0$, $B = \pi/2$ ($\theta_1 = \theta_3 = \pi/2$) and $\gamma = \pi/2$ to generate a binary phase-coded microwave signal and maximize its amplitude. The alternating current in Eq. (5) is expressed as

$$\begin{aligned} i_1(t) &= \frac{1}{4} R\alpha^2 E_0^2 \sin\left(\frac{\pi}{2} s(t)\right) \sin(\kappa \cos(\omega_s t)) \\ &\approx \frac{1}{2} R\alpha^2 E_0^2 \sin\left(\frac{\pi}{2} s(t)\right) [J_1(\kappa)\cos(\omega_s t) - J_3(\kappa)\cos(3\omega_s t)], \end{aligned} \quad (6)$$

where J_n is the nth-order Bessel function of the first kind. Under small signal modulation condition ($\kappa \ll 1$), the third harmonic is very small, and a binary phase-coded microwave signal at the fundamental frequency is generated, which is

$$i_{fundamental}(t) = \begin{cases} \frac{1}{2} R\alpha^2 E_0^2 J_1(\kappa)\cos(\omega_s t) & s(t) = 1 \\ \frac{1}{2} R\alpha^2 E_0^2 J_1(\kappa)\cos(\omega_s t + \pi) & s(t) = -1. \end{cases} \quad (7)$$

To generate a frequency-tripled phase-coded microwave signal, high modulation index ($J_1(\kappa) = 0$) is used to suppress the first harmonic, and the third harmonic will be in dominant, which can be expressed as

$$i_{tripled}(t) = \begin{cases} \frac{1}{2} R\alpha^2 E_0^2 J_3(\kappa)\cos(3\omega_s t + \pi) & s(t) = 1 \\ \frac{1}{2} R\alpha^2 E_0^2 J_3(\kappa)\cos(3\omega_s t) & s(t) = -1. \end{cases} \quad (8)$$

A frequency-tripled phase-coded microwave signal is generated.

When $\varphi_1 = \pi/2$ and $\varphi_2 = 0$, Eq. (4) can be simplified as

$$i(t) = \frac{1}{16} R\alpha^2 E_0^2 \left\{1 + 4\cos^2 A \cos^2(\gamma s(t) - B) + 4\cos A \cos(\gamma s(t) - B) \cos(\kappa \cos(\omega_s t))\right\}. \quad (9)$$

As can be seen from Eq. (9), at the output of the PD, only a DC and a baseband modulation product besides the microwave modulation term are generated, which has small difference with Eq. (5). We also set $A = 0$, $B = \pi/2$ ($\theta_1 = \theta_3 = \pi/2$) and $\gamma = \pi/2$ to generate a binary phase-coded microwave signal and maximize its amplitude. The microwave modulation term in Eq. (9) is expressed as

$$\begin{aligned} i_2(t) &= \frac{1}{4} R\alpha^2 E_0^2 \sin\left(\frac{\pi}{2} s(t)\right) \cos(\kappa \cos(\omega_s t)) \\ &\approx \frac{1}{4} R\alpha^2 E_0^2 \sin\left(\frac{\pi}{2} s(t)\right) [J_0(\kappa) - 2J_2(\kappa)\cos(2\omega_s t) + 2J_4(\kappa)\cos(4\omega_s t)]. \end{aligned} \quad (10)$$

In Eq. (10), there are a DC and two microwave terms. To generate a frequency-doubled phase-coded microwave signal, a small modulation index is selected to suppress the fourth harmonic. A binary phase-coded microwave signal at the doubled frequency is expressed as

$$i_{doubled}(t) = \begin{cases} \frac{1}{2} R\alpha^2 E_0^2 J_2(\kappa)\cos(2\omega_s t + \pi) & s(t) = 1 \\ \frac{1}{2} R\alpha^2 E_0^2 J_2(\kappa)\cos(2\omega_s t) & s(t) = -1. \end{cases} \quad (11)$$

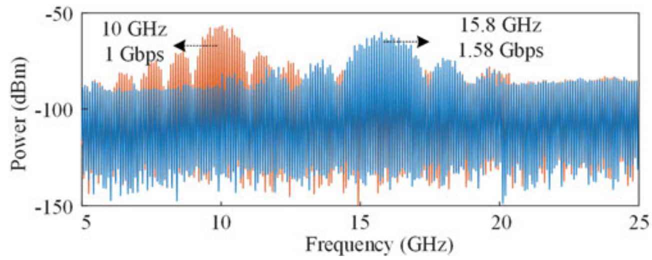

Fig. 2. Electrical spectra of the generated 10 GHz and 15.8 GHz binary phase-coded microwave signals at the fundamental frequency.

We can also increase the modulation index to suppress the second harmonic ($J_2(\kappa) = 0$). Under this condition, a frequency-quadrupled phase-coded microwave signal can be generated, which is expressed as

$$i_{quadrupled}(t) = \begin{cases} \frac{1}{2}R\alpha^2 E_0^2 J_4(\kappa)\cos(4\omega_s t) & s(t) = 1 \\ \frac{1}{2}R\alpha^2 E_0^2 J_4(\kappa)\cos(4\omega_s t + \pi) & s(t) = -1. \end{cases} \tag{12}$$

As discussed above, the proposed phase-coded microwave signal generator can generate a binary phase-coded microwave signal with a frequency multiplication factor from one to four under different system parameters. For the fundamental and frequency-doubled phase-coded microwave signal generation, the modulation index can be small, whereas for frequency-tripled and frequency-quadrupled phase-coded microwave signal generation, high modulation indices are required, which are $\kappa = 3.83$ and $\kappa = 5.13$, respectively. The corresponding voltages of the microwave reference signals applied to the DP-QPSK modulator are 1.22 V_π and 1.63 V_π.

3. Experimental Results and Discussion

An experiment based on the setup shown in Fig. 1(a) is performed. A light wave with an 18-dBm optical power generated from a LD (Teraxion-NLL) is injected into a DP-QPSK modulator (Fujitsu FTM7977). The DP-QPSK modulator has a 3-dB modulation bandwidth of 23 GHz and an insertion loss of 13 dB. The DP-QPSK modulator is driven by coding signals generated from a PPG (Anritsu MP1763C) and a microwave reference signal generated from a MSG (Agilent E8257D). The microwave reference signal is amplified by a PA before being applied to the modulator if a high modulation index is required. The optical signal at the output of the DP-QPSK modulator is amplified by an EDFA (Amonics) and then detected in a PD (u2t) with a 3-dB bandwidth of 40 GHz. The photocurrent at the output of the PD is then amplified by an EA with 20-dB gain. The spectra of the electrical signals are measured by a signal analyzer (Keysight N9010A), and the waveforms of the generated phase-coded microwave signals are monitored by a digital sampling oscilloscope (DSO, Agilent DCA-J 86100C).

First, we use small signal modulation index in the experiment to verify the generation of binary phase-coded microwave signals at the fundamental and doubled frequency. Fig. 2 shows the electrical spectra of two generated binary phase-coded microwave signals at the fundamental frequency with carrier frequencies of 10 GHz and 15.8 GHz. The data rates of the coding signals are 1 Gb/s and 1.58 Gb/s, respectively.

To study the performance of the generated phase-coded microwave signal, the coding signal applied to the DP-QPSK modulator is set as a "0101" sequence. The temporal waveforms of the generated 10-GHz and 15.8-GHz phase-coded microwave signals and the recovered phase information from the waveforms are shown in Fig. 3. As can be seen, the phase shifts between adjacent codes are very close to the theoretical value of 180 degrees.

Then, a pseudo-random bit sequence (PRBS) coding signal at 1 Gb/s or 1.58 Gb/s with a length of 64 bits generated from the PPG is applied to the DP-QPSK modulator. A waveform with a

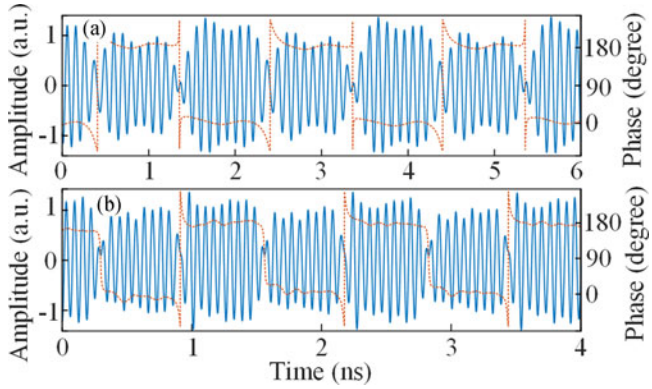

Fig. 3. Temporal waveforms of the generated fundamental binary phase-coded microwave signals with carrier frequencies at (a) 10 GHz and (b) 15.8 GHz. The dash lines are the recovered phase information from the waveforms.

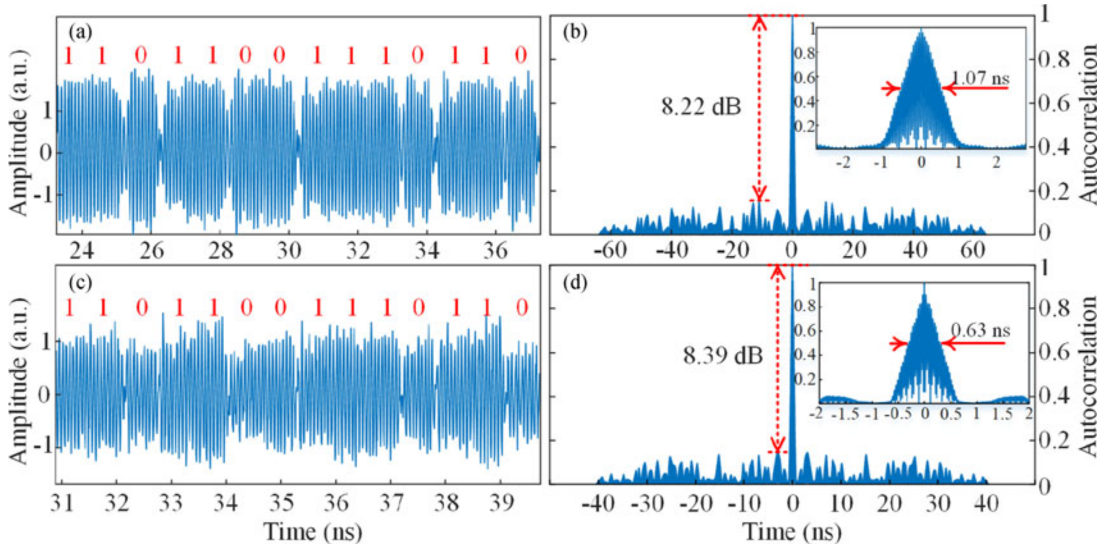

Fig. 4. (a) A section of the generated 64-bit binary phase-coded microwave signal at the fundamental frequency of 10 GHz. (b) Autocorrelation of the generated phase-coded microwave signal in (a). (c) A section of the generated 64-bit binary phase-coded microwave signal at the fundamental frequency of 15.8 GHz. (d) Autocorrelation of the generated phase-coded microwave signal in (c). The insets in (b) and (d) are the zoom-in views of the autocorrelation peaks.

time duration of 64 ns or 40.5 ns is generated, which is used to evaluate the pulse compression performance of the system. Fig. 4(a) shows a section (14 bits) of the generated 64-bit binary phase-coded microwave signal at the fundamental frequency of 10 GHz. The 64-bit binary phase-coded microwave signal is processed by Matlab to evaluate the pulse compression performance, which is shown in Fig. 4(b). A compressed pulse is generated with a peak-to-sidelobe ratio (PSR) of about 8.22 dB. Here the PSR is defined as the ratio of the mainlobe to the highest sidelobe. The inset in Fig. 4(b) shows the zoon-in view of the autocorrelation peak, which has a full width at half-maximum (FWHM) of about 1.07 ns, corresponding to a pulse compression ratio (PCR) of about 59.8. Here the PCR is defined as the ratio of the 3-dB temporal width of the transmitted pulse to that of the compressed pulse. Fig. 4(c) shows a section (14 bits) of the generated 64-bit binary phase-coded microwave signal at the fundamental frequency of 15.8 GHz. The compressed pulse is shown in Fig. 4(d), which has a PSR of about 8.39 dB and a PCR of about 64.3.

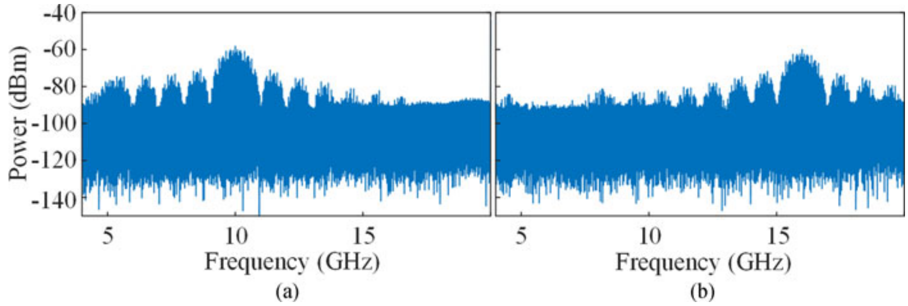

Fig. 5. Electrical spectra of the generated frequency-doubled phase-coded microwave signals with carrier frequencies at (a) 10 GHz and (b) 15.8 GHz.

It is well known that the Barker code can provide good autocorrelation performance, but only with a maximum code length of 13. If we use the 13-bit Barker code as the coding signal in the experiment, the PCR of the phase-coded microwave waveform is limited to 13. In order to generate phase-coded microwave signals with a lager PCR, 64-bit PRBS is used as the coding signal in the experiment. More importantly, the DSO and the PPG used in the experiment are the key reason why we do not use a Barker code. The PPG has a 1/64 clock output, which is used to trigger the DSO. If no additional frequency divider is used to divide the trigger from the PPG, the period of the coding signal should be 2^n ($n \leq 6$, n is an integer) so that the generated phase-coded microwave waveforms can be monitored by the DSO. If a Barker code is used, we can only choose 2-bit or 4-bit Barker code, which is so short that the PCR and PSR will both be 2 or 4. It has been proven that there are no further odd-length Barker codes, nor even-length Barker codes of $N < 10^{22}$. When the code length is longer than 13, the PRBS is more suitable to be the coding signal. The randomness of the PRBS determines that the PSR and the code length are not strictly proportional. However, if the code length is longer, it is more likely to get a larger PSR. The selection of the coding signal will greatly influence the pulse compression performance including the PCR and PSR. The code length defines the theoretical PCR of the generated phase-coded microwave signal, whereas different code patterns result in different theoretical PSRs. In the experiment, we use the longest code allowed by the test equipment, which is the 64-bit PRBS, to study the pulse compression performance of the generated phase-coded microwave signals. The 64-bit PRBS coding signal is optimized by choosing one sequence from many different 64-bit PRBSs using Matlab, which has the best PSR of about 8.52 dB in the simulation among all the code patterns. In addition, if a real time oscilloscope is used in the experiment, there is no such code length restriction. The coding signals with arbitrary length can be used and the generated phase-coded microwave waveforms can be monitored by the real time oscilloscope.

Then, frequency-doubled phase-coded microwave signal generation is studied. As discussed in Section 2, a small modulation index is enough to generate a frequency-doubled phase-coded microwave signal. Fig. 5 shows the electrical spectra of the generated binary phase-coded microwave signals at the doubled frequency. Two specific cases with microwave reference frequencies of 5 GHz and 7.9 GHz are shown in Fig. 5(a) and (b), respectively. The data rates of the coding signals in the measured spectra in Fig. 5 are both 1 Gb/s. By properly controlling the parameters in the system, only frequency-doubled phase-coded microwave signals at 10 GHz and 15.8 GHz are generated.

The performance of the generated frequency-doubled phase-coded microwave signal is also studied. The coding signal is set as a “0101” sequence with a data rate of 1 Gb/s or 1.58 Gb/s when the carrier frequency of the generated phase-coded microwave signal is 10 GHz or 15.8 GHz. The temporal waveforms of the generated 10-GHz and 15.8-GHz frequency-doubled phase-coded microwave signals and the recovered phase information from the waveforms are shown in Fig. 6. The phase shifts between adjacent codes are very close to the theoretical value of 180 degrees. The pulse compression performance is also studied, which is shown in Fig. 7. The 10-GHz

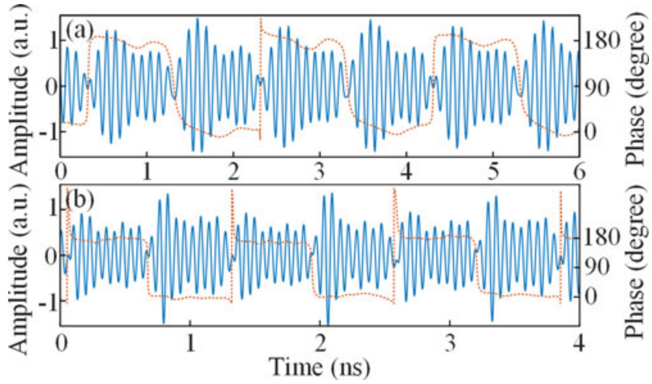

Fig. 6. Temporal waveforms of the generated frequency-doubled binary phase-coded microwave signals with carrier frequencies at (a) 10 GHz and (b) 15.8 GHz. The dash lines are the recovered phase information from the waveforms.

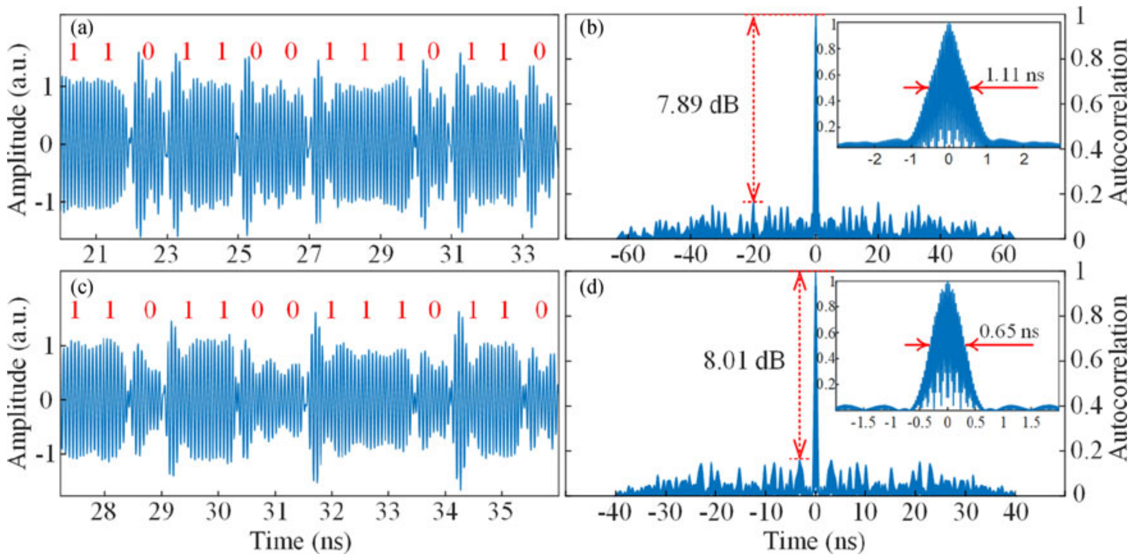

Fig. 7. (a) A section of the generated 64-bit frequency-doubled binary phase-coded microwave signal at 10 GHz. (b) Autocorrelation of the generated phase-coded microwave signal in (a). (c) A section of the generated 64-bit frequency-doubled binary phase-coded microwave signal at 15.8 GHz. (d) Autocorrelation of the generated phase-coded microwave signal in (c). The insets in (b) and (d) are the zoom-in views of the autocorrelation peaks.

phase-coded microwave signal has a PSR of about 7.89 dB and a PCR of about 57.7, whereas the 15.8 GHz phase-coded microwave signal has a PSR of about 8.01 dB and a PCR of about 62.3.

Then, frequency-tripled phase-coded microwave signal generation is demonstrated. In the experiment, we use a high power amplifier, which can provide an output power up to 1 W to achieve the required modulation index. Fig. 8 shows two specific cases, where the frequencies of the microwave reference signals are 3.33 GHz and 5.3 GHz, and the corresponding data rates of the coding signals are 0.999 Gb/s or 1.59 Gb/s. As shown in Fig. 8, a frequency-tripled phase-coded microwave signal centered at 9.99 GHz or 15.9 GHz is generated, and the first, second and fourth harmonics are suppressed with a suppression ratio of more than 15 dB or 14 dB. The fifth harmonic has a relatively higher power level because in the experiment we use high modulation index. However, the fifth harmonics can be suppressed by using a EA or a PD with limited response bandwidth. The 14 dB or 15 dB suppression ratio in the experiment may be not high enough for practical

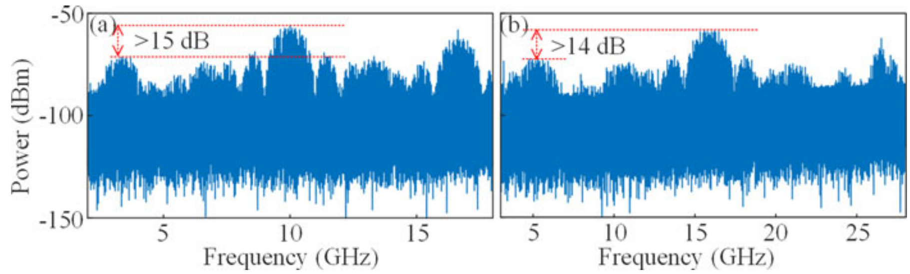

Fig. 8. Electrical spectra of the generated frequency-tripled phase-coded microwave signals with carrier frequencies at (a) 9.99 GHz and (b) 15.9 GHz.

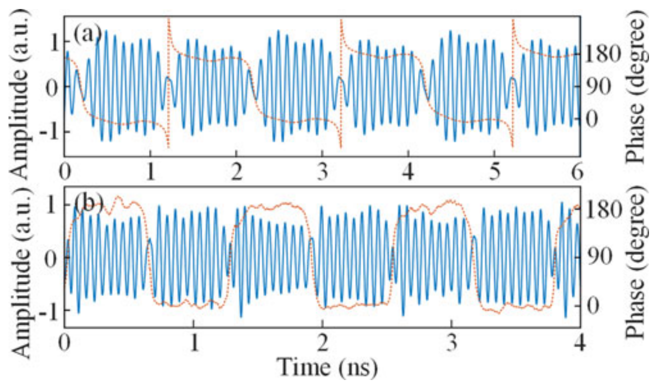

Fig. 9. Temporal waveforms of the generated frequency-tripled binary phase-coded microwave signals with carrier frequencies at (a) 9.99 GHz and (b) 15.9 GHz. The dash lines are the recovered phase information from the waveforms.

applications. The suppression ratio can be further increased if precise bias points are controlled and maintained by using bias control circuits.

To verify the performance of the binary phase-coded microwave signal, the coding signal is set as a "0101" sequence. The temporal waveforms of the generated phase-coded microwave signals are shown in Fig. 9 in solid lines, and the recovered phase information using Hilbert transform is in red dash lines. It is obvious that there are phase jumps in the waveforms, and 180-degree phase shifts are obtained from the recovered phase information. Fig. 10(a) and (c) show a section (14 bits) of the generated pulse compression signals. Fig. 10(b) and (d) show the autocorrelations of the pulse compression signals. For the 9.99 GHz phase-coded microwave signal, a PSR of about 8.50 dB and a PCR of about 58.2 are obtained. For the 15.9 GHz phase-coded microwave signal, the PSR is about 7.46 dB and the PCR is about 59.2.

Then, frequency-quadrupled phase-coded microwave signal generation is demonstrated. Theoretically, the required voltage of the microwave reference signal is 5.71 V when a DP-QPSK modulator with a 3.5 V half-wave voltage is used in the experiment. The 5.71 V amplitude of the applied microwave signal slightly exceeds the maximum allowable voltage of the DP-QPSK modulator. Furthermore, the attenuation of the transmission cables and adapters used in the experiment also makes it difficult to achieve 5.71 V input voltage to the DP-QPSK modulator, so we use a high modulation index slightly lower than the theoretical value in the experiment.

Fig. 11 shows two specific cases of the spectra of the generated frequency-quadrupled phase-coded microwave signals, where the frequencies of microwave reference signals are 2.5 GHz and 3.95 GHz, and the corresponding data rates of the coding signals are 1 Gb/s and 1.58 Gb/s, respectively. Since the modulation index is not high enough in the experiment, the frequency components at the doubled frequency are not suppressed, which is higher than the desired signals at the quadrupled frequency. Signals at the sextupled frequency are also observed due to the use

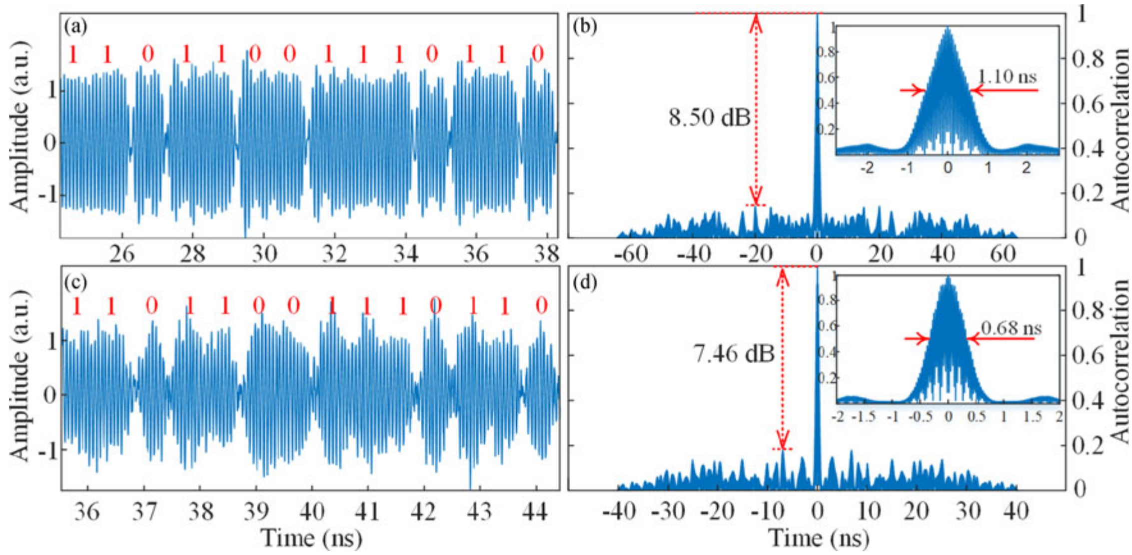

Fig. 10. (a) A section of the generated 64-bit frequency-tripled binary phase-coded microwave signal at 9.99 GHz. (b) Autocorrelation of the generated phase-coded microwave signal in (a). (c) A section of the generated 64-bit frequency-tripled binary phase-coded microwave signal at 15.9 GHz. (d) Autocorrelation of the generated phase-coded microwave signal in (c). The insets in (b) and (d) are the zoom-in views of the autocorrelation peaks.

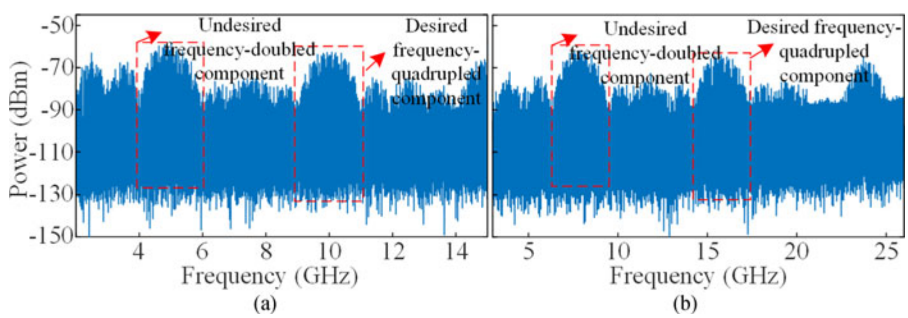

Fig. 11. Electrical spectra of the generated frequency-quadrupled phase-coded microwave signals with carrier frequencies at (a) 10 GHz and (b) 15.8 GHz.

of the high modulation index. In the experiment, we use an electrical band-pass filter to get the desired frequency-quadrupled phase-coded microwave signals.

To verify the performance of the generated phase-coded microwave signal, the coding signal applied to the DP-QPSK modulator is set as a “0101” sequence. Fig. 12 shows the temporal waveforms of the generated frequency-quadrupled phase-coded microwave signals with carrier frequencies of 10 GHz and 15.8 GHz. The recovered phase information using Hilbert transform is in red dash lines. It is obvious that there are phase jumps in the waveforms, and 180-degree phase shifts are obtained from the recovered phase information. The pulse compression performance for the generated frequency-quadrupled phase-coded microwave signals is also investigated. 14 bits of the generated phase-coded microwave signals are shown in Fig. 13(a) and (c). From the autocorrelations of the phase-coded microwave signals shown in Fig. 13(b) and (d), the 10-GHz frequency-quadrupled phase-coded microwave signal has a PSR of about 8.31 dB and a PCR of 55.6, whereas the PSR and PCR for the 15.8-GHz frequency-quadrupled phase-coded microwave signal are 7.69 dB and 59.6.

To study the robustness of the generated phase-coded microwave signals to noise, an additional white Gaussian noise (AWGN) is added to the generated waveforms. Fig. 14 shows a section of the 9.99-GHz frequency-tripled microwave waveform with an AWGN and the corresponding pulse

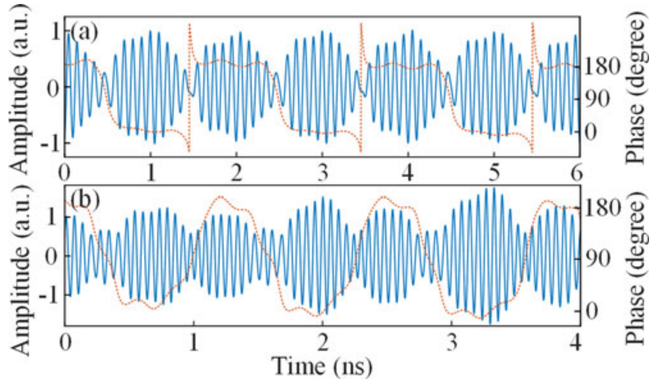

Fig. 12. Temporal waveforms of the generated frequency-quadrupled binary phase-coded microwave signals with carrier frequencies at (a) 10 GHz and (b) 15.8 GHz. The dash lines are the recovered phase information from the waveforms.

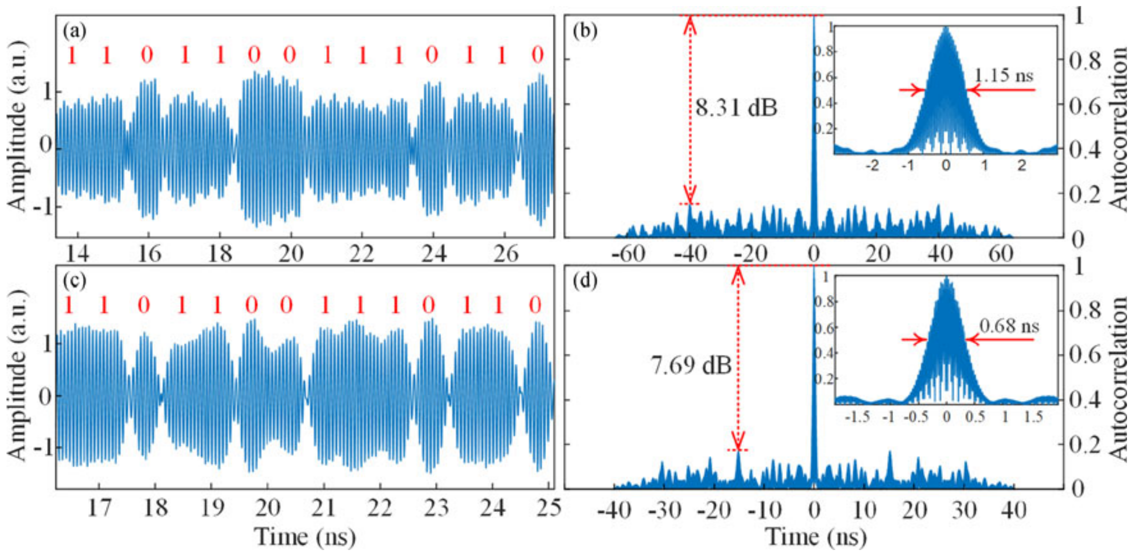

Fig. 13. (a) A section of the generated 64-bit frequency-quadrupled binary phase-coded microwave signal at 10 GHz. (b) Autocorrelation of the generated phase-coded microwave signal in (a). (c) A section of the generated 64-bit frequency-quadrupled binary phase-coded microwave signal at 15.8 GHz. (d) Autocorrelation of the generated phase-coded microwave signal in (c). The insets in (b) and (d) are the zoom-in views of the autocorrelation peaks.

compression performance. As can be seen from the original waveform in Fig. 10(a), the sinusoidal waveform and the phase jumps between adjacent codes are distinguishable from the temporal waveform, which means the generated phase-coded microwave signal has good signal-to-noise ratio (SNR). An AWGN is generated and added to the phase-coded microwave signal, where the SNR is controlled to be -10 dB. The noisy waveform is shown in Fig. 14(a), where the sinusoidal waveform and the phase jumps cannot be distinguished. Fig. 14(b) shows the correlation of the noisy waveform in Fig. 14(a) and the original waveform in Fig. 10(a). The PSR is 7.55 dB and the PCR is 54.8. Compared with the result in Fig. 10(b), very small performance degradation is observed. Furthermore, the power of the AWGN is increased to lower the SNR to -20 dB, and the obtained waveform is shown in Fig. 14(c). The pulse compression performance in this case is shown in Fig. 14(d). Since the power of the AWGN is too large, the PSR decreases to about 5.36 dB, whereas the PCR does not have obvious degradation. Same results are also obtained when the fundamental, frequency-doubled or frequency-quadrupled phase-coded microwave signal

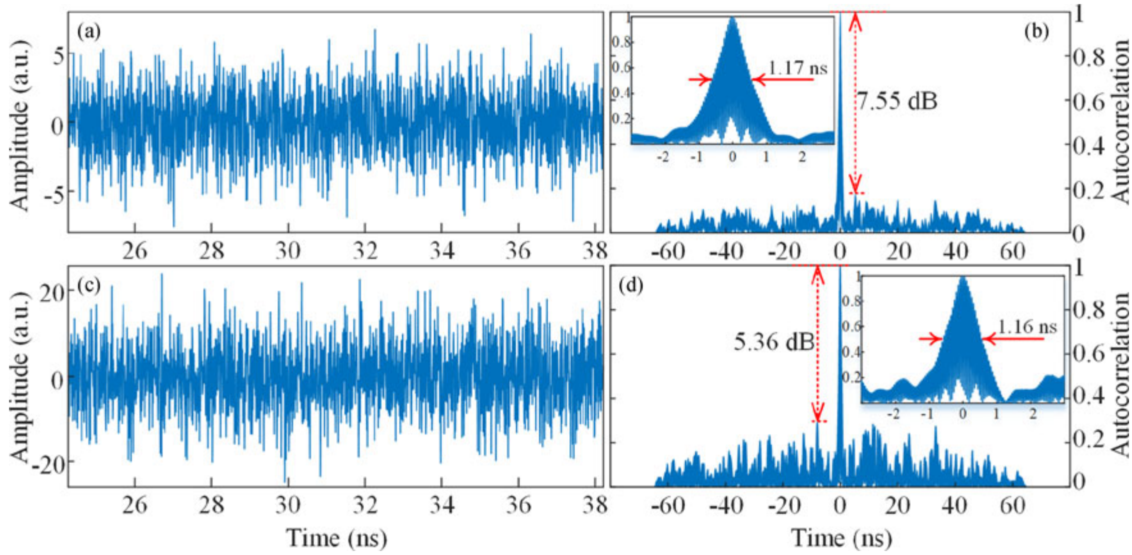

Fig. 14. (a) A section of the generated 64-bit frequency-tripled binary phase-coded microwave signal at 9.99 GHz with an AWGN, the SNR is −10 dB. (b) Correlation of the original phase-coded microwave signal and the noisy signal in (a). (c) A section of the generated 64-bit frequency-tripled binary phase-coded microwave signal at 9.99 GHz with an AWGN, the SNR is −20 dB. (d) Correlation of the original phase-coded microwave signal and the noisy signal in (c). The insets in (b) and (d) are the zoom-in views of the correlation peaks.

is used. The results above confirm that the phase-coded microwave signal generated using the proposed approach has very good robustness to noise.

As shown in the experimental results above, using the compact structure mainly consisting of a DP-QPSK modulator and a single-port PD, binary phase-coded microwave signals at the fundamental frequency, the doubled frequency, the tripled frequency and the quadrupled frequency can be generated. In the proof-of-concept experiment, the frequencies of the reference signals are located from 2.5 GHz to 15.8 GHz, which is limited by the bandwidth of the EA used in the experiment. The frequency of the microwave reference signal can be increased up to more than 23 GHz with a DP-QPSK modulator having a 3-dB bandwidth of 23 GHz, which means the frequency of the generated phase-coded microwave signal can reach more than 92 GHz when PD and EA with enough bandwidth are employed. For the coding signal, the DP-QPSK modulator has a modulation speed of up to 31.4 Gbaud, so the data rate of the coding signal can be up to 31.4 Gb/s.

It is also noticed that the PCR and PSR performance of the generated phase-coded microwave signals is very close to the theoretical values of 64 and 8.52 dB defined by the selected coding signal. However, there are still some performance differences, which are caused by many factors, such as the non-ideal bias points of the modulator, the noise in the microwave photonic system and the non-ideal polarization control and alignment, and so on. Among these factors, the non-ideal bias points play an important role. For the accurate and stable operation of the system, six bias voltages of the modulator should be carefully controlled and maintained. In our experiment, the bias voltages are supplied by DC power supplies with no feedback control, which makes the exact bias points very difficult to be maintained in very long-term operation. The performance of the generated signals will degrade due to the drifts of bias points. This is why the PCRs and PSRs obtained from the experiment have some performance difference with the theoretical values in some cases. In practical applications, commercially available bias control circuits can be employed to stabilize the bias points of the modulator, which will guarantee stable operation during very long-term operation.

As discussed in the theory, the voltages of the applied microwave signals for frequency-tripled and frequency-quadrupled phase-coded microwave signal generation are 1.22 V_π and 1.63 V_π, respectively. The V_π of the DP-QPSK modulator is 3.5 V, so the corresponding voltages are 4.27 V and 5.71 V. When the impendence is 50 Ω, the power of the applied microwave signals is 22.6 dBm and 25.1 dBm, so the total power from the PA should be 25.6 dBm and 28.1 dBm. However, because the transmission cables and adapters used in the experiment have certain losses, the actual power from the PA should be higher than the theoretical values. This is why using a 1 W (30 dBm) PA cannot obtain the expected result for frequency-quadrupled phase-coded microwave signal generation. As shown in Fig. 11, the second harmonic is even higher than the desired frequency-quadrupled component. However, the method for a pure frequency-quadrupled phase-coded microwave signal generation is theoretically established, which can be proved by the eliminating of the first and third harmonic in Fig. 11. By filtering out the frequency-quadrupled phase-coded microwave signal, its performance is as good as that of the fundamental, frequency-doubled or frequency-tripled phase-coded microwave signal. Different from the frequency-quadrupled phase-coded microwave signal generation, the frequency-tripled phase-coded microwave signal is generated as predicted because of its relatively lower required voltage of the applied microwave signal, where the frequency-tripled component is in dominant and other harmonics are suppressed. In practical applications, the feeder lines can be shortened by the mature electronic technique, so that the insertion loss can be reduced. If the insertion loss of the feeder line is controlled at less than 1.9 dB, the 1 W PA can meet the needs of the frequency-quadrupled phase-coded microwave signal generation, so that the electrical band-pass filter used in our experiment can be removed.

The contribution of the proposed technique in this paper is that it can realize tunable frequency multiplication factor from one to four, and the frequency of the generated phase-coded microwave signal can be tuned in a large frequency range. The proposed system has a relatively simple structure, but the power consumption may be higher than the previous work, when large frequency multiplication factor is desired. However, it is expected that DP-QPSK modulators with lower half-wave voltage are fabricated, or such modulators are implemented by integrated photonics, so that the required power of the applied microwave signal can be decreased, resulting in a lower power consumption.

4. Conclusion

In conclusion, a novel frequency-tunable binary phase-coded microwave signal generator with a tunable frequency multiplication factor is proposed and experimentally investigated. The key contribution of the work is that fundamental, frequency-doubled, frequency-tripled or frequency-quadrupled phase-coded microwave signal can be generated using a compact and reconfigurable structure, which mainly consists of a DP-QPSK modulator and a single-port PD, and the frequency of the generated phase-coded microwave signal can be tuned in a large frequency range. A proof-of-concept experiment is performed. The generation of a phase-coded microwave signal at the fundamental frequency, doubled frequency, tripled frequency or quadrupled frequency is demonstrated. The frequency tunability as well as the pulse compression performance of the proposed system is also investigated. The proposed technique is expected to find applications in high-frequency or multifunction radar systems.

References

[1] M. Skolnik, "Role of radar in microwaves," *IEEE Trans. Microw. Theory Techn.*, vol. 50, no. 3, pp. 625–632, Aug. 2002.
[2] M. Cohen, "Pulse compression in radar systems," in *Principles of Modern Radar*. New York, NY, USA: Springer, 1987, pp. 465–501.
[3] P. Ghelfi *et al.*, "A fully photonics-based coherent radar system," *Nature*, vol. 507, no. 7492, pp. 341–345, Mar. 2014.
[4] J. Yao, "Microwave photonics," *J. Lightw. Technol.*, vol. 27, no. 3, pp. 314–335, Feb. 2009.
[5] D. Marpaung, C. Roeloffzen, R. Heideman, A. Leinse, S. Sales, and J. Capmany, "Integrated microwave photonics," *Laser Photon. Rev.*, vol. 7, no. 4, pp. 506–538, Jul. 2013.
[6] J. McKinney, D. Leaird, and A. Weiner, "Millimeter-wave arbitrary waveform generation with a direct space-to-time pulse shaper," *Opt. Lett.*, vol. 27, no. 15, pp. 1345–1347, Aug. 2002.
[7] A. Weiner, "Ultrafast optical pulse shaping: A tutorial review," *Opt. Commun.*, vol. 284, no. 15, pp. 3669–3692, Jul. 2011.

[8] H. Chi and J. P. Yao, “All-fiber chirped microwave pulse generation based on spectral shaping and wavelength-to-time conversion,” *IEEE Trans. Microw. Theory Techn.*, vol. 55, no. 9, pp. 1958–1963, Sep. 2007.

[9] Z. Tang, T. Zhang, F. Zhang, and S. Pan, “Photonic generation of a phase-coded microwave signal based on a single dual-drive Mach–Zehnder modulator,” *Opt. Lett.*, vol. 38, no. 24, pp. 5365–5368, Dec. 2013.

[10] W. Li, L. Wang, M. Li, H. Wang, and N. Zhu, “Photonic generation of binary phase-coded microwave signals with large frequency tunability using a dual-parallel Mach–Zehnder modulator,” *IEEE Photon. J.*, vol. 5, no. 4, Aug. 2013, Art. no. 5501507.

[11] Y. Chen, A. Wen, and J. Yao, “Photonic generation of frequency tunable binary phase-coded microwave waveforms,” *IEEE Photon. Technol. Lett.*, vol. 25, no. 23, pp. 2319–2322, Oct. 2013.

[12] X. Li, S. Zhao, S. Pan, Z. Zhu, K. Qu, and T. Lin, “Generation of a frequency-quadrupled phase-coded signal using optical carrier phase shifting and balanced detection,” *Appl. Opt.*, vol. 56, no. 4, pp. 1151–1156, Feb. 2017.

[13] Z. Li, W. Li, H. Chi, X. Zhang, and J. Yao, “Photonic generation of phase-coded microwave signal with large frequency tunability,” *IEEE Photon. Technol. Lett.*, vol. 23, no. 11, pp. 712–714, Mar. 2011.

[14] H. Jiang, L. Yan, J. Ye, W. Pan, B. Luo, and X. Zou, “Photonic generation of phase-coded microwave signals with tunable carrier frequency,” *Opt. Lett.*, vol. 38, no. 8, pp. 1361–1363, Apr. 2013.

[15] Z. Li, M. Li, H. Chi, X. Zhang, and J. Yao, “Photonic generation of phase-coded millimeter-wave signal with large frequency tunability using a polarization-maintaining fiber Bragg grating,” *IEEE Microw. Wireless Compon. Lett.*, vol. 21, no. 12, pp. 694–696, Oct. 2011.

[16] S. Liu, D. Zhu, Z. Wei, and S. Pan, “Photonic generation of widely tunable phase-coded microwave signals based on a dual-parallel polarization modulator,” *Opt. Lett.*, vol. 39, no. 13, pp. 3958–3961, Jul. 2014.

[17] Y. Zhang, F. Zhang, and S. Pan, “Generation of frequency-multiplied and phase-coded signal using an optical polarization division multiplexing modulator,” *IEEE Trans. Microw. Theory Techn.*, vol. 65, no. 2, pp. 651–660, Feb. 2017.

[18] Y. Chen, A. Wen, and W. Zhang, “Generation of phase-coded microwave signals through equivalent phase modulation,” *IEEE Photon. Technol. Lett.*, vol. 29, no. 16, pp. 1371–1374, Aug. 2017.

[19] X. Li, J. Yu, and G. Chang, “Frequency-quadrupling vector mm-wave signal generation by only one single-drive MZM,” *IEEE Photon. Technol. Lett.*, vol. 28, no. 12, pp. 1302–1305, Jun. 2016.

[20] X. Li, J. Xiao, and J. Yu, “W-band vector millimeter-wave signal generation based on phase modulator with photonic frequency quadrupling and precoding,” *J. Lightw. Technol.*, vol. 35, no. 13, pp. 2548–2558, Jul. 2017.